ELEMENTA
Science of the Anthropocene

Mustaffa, NIH, et al 2017 High-resolution variability of the enrichment of fluorescence dissolved organic matter in the sea surface microlayer of an upwelling region. *Elem Sci Anth*, 5: 52, DOI: https://doi.org/10.1525/elementa.242

RESEARCH ARTICLE

High-resolution variability of the enrichment of fluorescence dissolved organic matter in the sea surface microlayer of an upwelling region

Nur Ili Hamizah Mustaffa, Mariana Ribas-Ribas and Oliver Wurl

Enrichment of fluorescence dissolved organic matter (FDOM) in the sea surface microlayer (SML) provides insights into biogeochemical processes occurring at the sea surface, including cycling of organic matter, photochemistry, and air-sea gas exchange. We present data concerning the variability of FDOM enrichment in the SML during upwelling events in the Baltic Sea (Cruise M117). Our results show that FDOM is frequently enriched (75% of all samples) and that enrichment factors are significantly higher in SMLs located in regions with upwelling (pooled median = 1.4) compared to a non-upwelling region (median = 1.1). The enrichment factor of FDOM showed short time-scale variability, changing by 6% within ten-minute intervals. Larger variabilities (standard deviation up to ±0.14 μg L^{-1} compared to background of ±0.01 μg L^{-1}) occurred when fronts were present and when the SML was mixed with underlying bulk water. Small-scale patchiness, indicated by changes in the variability of FDOM enrichment in SML, was a common feature of the sea surface. Wind speed played a potential role in controlling the enrichment of FDOM in the SML, but the effects of solar radiation on photochemical processes, mixing and upwelling of water masses, and biological processes as a source of FDOM also influence enrichment at this critical interface between ocean and atmosphere.

Keywords: sea surface microlayer; fluorescence dissolved organic matter; spatiotemporial variability; upwelling; surface renewal

1. Introduction

The uppermost part of the ocean, covering approximately 70% of the surface is defined as the sea surface microlayer (SML) (Liss and Duce, 2005). Due to its unique position between the atmosphere and ocean, the SML plays an important role in biogeochemical processes, including the marine carbon cycle, photochemistry and air-sea exchange of climate-relevant gases. All materials exchanged between the ocean and atmosphere, including gases, particulate organic matter, and sea salt, have to pass through the SML (Liss and Duce, 2005). With a total thickness between 1 μm and 1000 μm, depending on the sampling technique (Shinki et al., 2012) and region of interest (Hardy, 1982), the SML remains sufficiently stable at a global average wind speed of 6.6 m s^{-1} (Wurl et al., 2011b) to control the rate of air-sea exchange of gases and heat, highlighting its global relevance. It is well established that the SML has unique physical, chemical, and biological properties that differ from those of the well-mixed underlying water masses (Hardy, 1982; Cunliffe et al., 2013). Biological and physical processes in the water column, such as primary productivity, diffusion, buoyancy flux, and rising bubbles, are the main factors determining the enrichment of chemical compounds and microbes in the SML (Wurl et al., 2009; Stolle et al., 2010). Enriched materials include surface-active dissolved organic matter (DOM) (e.g., carbohydrates, proteins and lipids) and particulate organic matter (POM), as well as autotrophic and heterotrophic cells (Williams et al., 1986; Cunliffe et al., 2009). Fluorescence dissolved organic matter (FDOM) is a fraction of chromophoric DOM (CDOM) which not only absorbs but also emits a blue fluorescence when it is irradiated with ultraviolet (UV) light (Coble, 2007). FDOM is often used as an indicator for humic-like marine DOM (Yamashita and Tanoue, 2009) and frequently enriched in the SML (Zhang and Yang, 2013) due to its hydrophobic properties.

CDOM enrichment in the SML is of particular interest due to its active role in photochemistry (de Bruyn et al., 2011), as the SML is the part of the ocean with the highest exposure to radiation. For this reason, some photochemical reactions in the SML can be unique (Carlson, 1993), and the SML may act as microreactor (Blough, 2005), including changing the composition of surface active species

Institute for Chemistry and Biology of the Marine Environment, Carl Von Ossietzky Universität Oldenburg, 26382 Wilhelmshaven, DE

Corresponding author: Nur Ili Hamizah Mustaffa (iliehamizah@gmail.com)

and, therefore, potentially altering wave damping and gas exchange rates. Recently, Galgani and Engel (2016) reported that CDOM enrichment in the SML within an upwelling region can be an indicator of photochemical processes and microbial alteration of DOM. Cell lysis, a response to extreme light exposure within the SML, and exudation processes release DOM directly into the air-sea boundary layer (Tilstone et al., 2010) where it may become a source of CDOM/FDOM for the underlying water masses. Moreover, the continuous photochemical alteration of DOM results in the formation of biologically labile compounds (i.e., pyruvate) replenishing the DOM pool for biological utilization (Kieber et al., 1989). Upwelling brings up cooler, nutrient- and DOM-enriched deep water to the surface through Ekman pumping (Clemente-Colon and Xiao-Hai, 1999). This process continuously supplies organic matter to the SML.

Physical parameters such as high salinity, temperature, wind force, solar and UV radiation also control the enrichment of DOM in the SML. In particular, wind speed and primary productivity play a crucial role in the enrichment of surface-active DOM (Wurl et al., 2011b). At low wind speeds, surface enrichment can be sustained through diffusive transport of surface-active compounds due to the stability of the SML. At moderate to high wind speeds, breaking waves will disrupt the surface and physically force enriched DOM back to the bulk water, resulting in low surface enrichment (Frew et al., 2004). However, breaking waves also aerate the bulk water, and rising air bubbles become an upward transport mechanism for the dispersed surface-active DOM; Wurl et al. (2011b) observed enrichment of organic matter in the SML when wind speed increased up to 10 m s^{-1}. Solar and UV radiation drive photochemical reactions, acting as the source or sink of CDOM in the SML (Tilstone et al., 2010; Galgani and Engel, 2016). Yu (2010) modeled sea surface salinity based on evaporation and heat flux, finding that increased density causes SML water to sink and therefore frequently renew the surface with bulk water. The SML can be re-established within seconds after disruption (Dragcevic and Pravdic, 1981), such as breaking waves and surface renewal. The complex process of DOM enrichment and its important role in the formation of the SML may lead to patchiness of the air-sea boundary layer.

Frew et al. (2002) reported that small-scale variability (10–1000 m) of CDOM fluorescence results in complex patterns of its enrichment in the SML. Additionally, the authors pointed out that these small-scale changes in surface enrichment are often associated with wind speed and wave slope. Later, Frew et al. (2004) described the variability of CDOM fluorescence enrichment at larger scales (10–1000 km) and showed that this variability was related to the presence of different water masses with various sources of surface-active materials. Overall, the short time-scale variability of enrichment processes in the SML is not well understood due to observational challenges, but is important for obtaining a better understanding of air-sea interactions potentially controlled by patchy enrichment of surface-active DOM.

The primary aim of this study was to understand the spatiotemporal variability in FDOM enrichment in the SML through high-resolution observations. The influence of upwelling, biological activities, and meteorological forces on the enrichment process was investigated. Details regarding the patchiness of SML distribution are also provided.

2. Materials and methods

2.1 Study area

Field measurements were conducted in the Baltic Sea onboard the R/V *Meteor* (cruise M117, July 23 to August 17, 2015) at the sampling locations shown in **Figure 1**. In order to identify variability in FDOM enrichment during upwelling and non-upwelling events, four stations were chosen: one upwelling station (UP3), two stations within an area influenced by upwelling (UP2 and UP4), and one non-upwelling station (TF0271). An upwelling event was observed off the island Öland (Sweden), causing a temperature difference of 3.671°C between the UP3 and UP4 stations, and 7.498°C between the UP3 and TF0271 stations. FDOM concentrations and supporting data (e.g., salinity and temperature) for the UP2 and UP3 stations have been published elsewhere (Ribas-Ribas et al., 2017). Here we report data from stations UP2 and TF0271 and consider the spatial and temporal variabilities associated with all four stations.

2.2 Field measurements

A state-of-the-art research catamaran (Ribas-Ribas et al., 2017) was deployed to measure *in situ* biogeochemical parameters with high resolution (every ten seconds). The SML samples were collected using six rotating glass discs (diameter 60 cm, thickness 0.8 cm) mounted on

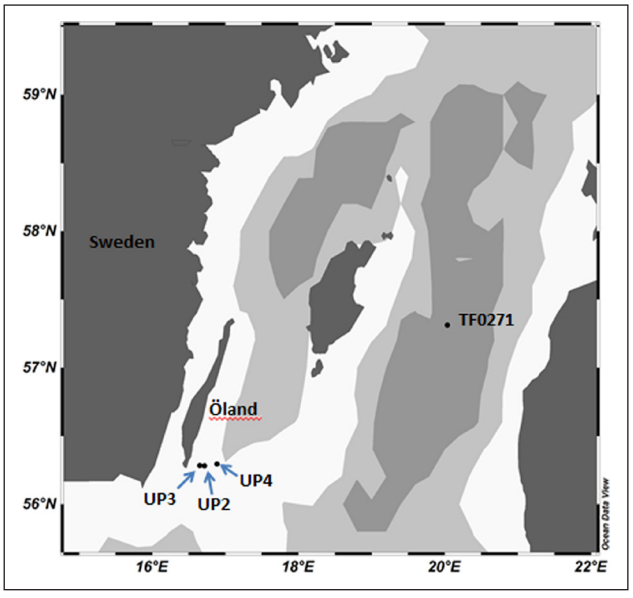

Figure 1: Map of sampling stations. UP3 is the upwelling station and UP2 and UP4 are influenced by upwelling, while TF0271 is located in a non-upwelling region. Map was created using Ocean Data View. DOI: https://doi.org/10.1525/elementa.242.f1

a research catamaran. The glass discs were submerged approximately 15 cm into the water and rotated with seven rotations per minute. The SML adheres to the discs through the phenomenon of surface tension on the ascending side; it is wiped off by a set of polycarbonate wipers mounted on the descending side between the discs. Using this technique, we were able to collect 20L of the SML within one hour and with a thickness of about 50–80 μm (Shinki et al., 2012), which is in line with the SML thicknesses of 50 ± 10 μm using pH microelectrodes (Zhang et al., 2003). The thickness of collected SML was estimated from the area of the discs, rotations per minute, collected volume and length of sampling time. Bulk water was sampled simultaneously with the SML using polypropylene tubing at one-meter depth. FDOM of SML and bulk water was measured simultaneously using a flow-through system with two microFlu-CDOM fluorometers (TriOS GmbH, Germany). The microFlu-CDOM uses a UV-LED with a maximum excitation light spectrum of 370 nm as an excitation wavelength source. Emission wavelength is measured at 460 nm with full width at half maximum (FWHM) of 100 nm. The outputs of the two sensors (0–5 volts DC) were recorded by a two-channel data logger (Track-IT™, Monarch Instruments, USA). The sensors were calibrated by the supplier using a standard solution of quinine sulfate dehydrate in 0.05 M sulfuric acid, and scaling factors were stored internally. The scaling factor from the calibration was used to transform the raw fluorescence reading to FDOM concentration (μg L^{-1}). The blank measurement was made before every deployment for quality control. The ultra-pure water was pumped through the flow-through system for several minutes and the real-time data of the blank were noted. The average of blank was 2.2 ± 0.5 μg L^{-1} (n = 10).

We recorded high-precision temperatures (HPT) at depths of approximately 2 cm and 15 cm, as required to evaluate mixing, using a two-channel P-795 temperature logger (Dostmann Electronic, Germany). The salinity and temperature of both the SML and bulk water were measured simultaneously using two multi-parameter devices (Model: PCD 650, Eutech Instrument, Singapore). Chlorophyll *a* (Chl *a*) and the quantum efficiency of the phytoplankton community in the bulk water were monitored using an active fluorometer, PhytoFlash (Turner Designs, Sunnyvale, CA, USA). The PhytoFlash detection system uses three low-intensity LEDs to monitor minimum florescence (F_o), maximum fluorescence (F_m), and variable fluorescence (F_v; $F_m - F_o$). Quantum efficiency, also known as yield (F_v/F_m), determines how well phytoplankton can assimilate light for photosynthesis. Before and after the cruise, the PhytoFlash was calibrated with reference measurements on a benchtop fluorometer according to the supplier's recommendation. All biogeochemical parameters were recorded and time-synchronized every ten seconds. Meteorological data, including wind speed, solar radiation (measured wavelength: 400–1100 nm), and UV index (measured wavelength: 250–400 nm) were recorded at one-minute intervals using a Vintage Pro2 weather station (Davis Instruments, USA).

2.3 Laboratory analysis

The Chl *a* concentration in discrete samples from the bulk water was analyzed using a fluorimeter, in line with Lorenzen (1967). After collection, the samples with a volume of 500 mL were immediately filtered under a vacuum onto GF/F filters (25 mm, Whatman, UK) and stored at –80°C prior to extraction. The filters were placed in 20 mL vials with 8 mL of 90% acetone. The filters were kept at 4°C in the dark for 24 hours before measurement using a fluorimeter (Model: Jenway 6285, Bibby Scientific Ltd, UK). Prior to analysis, the fluorimeter was calibrated with pure Chl *a* extracted from spinach (Sigma Aldrich, Germany). The concentration of surfactants in the SML and bulk samples was measured using phase-sensitive alternating voltammetry (Model: VA 747, Methrom, Switzerland) with a hanging mercury drop electrode (Ćosović and Vojvodić, 1998) and expressed as the equivalent concentration of the non-ionic surfactant Triton X-100 (Teq), as in Wurl et al. (2009). Unfiltered samples (10 mL) were measured using a standard addition technique. Each sample was measured three or four times, resulting in relative standard deviations below 6%.

2.4 Data and statistical analysis

Statistical analysis was performed with GraphPad PRISM 5.0 and Origin Pro version 8.5. The enrichment factor (EF) for FDOM was calculated as the ratio of the FDOM concentration in the SML to that of the corresponding bulk sample (one-meter depth). The non-parametric test (Mann-Whitney test) was performed to determine whether the enrichment of FDOM differs significantly between upwelling and non-upwelling regions. Differences were considered to be significant when $p \leq 0.05$ with a 95% confidence level. The correlation test is based on Spearman's correlation. Wind was grouped into three regimes, in line with Wurl et al. (2011b), based on the Pierson–Moskowitz sea spectrum (Pierson and Moskowitz, 1964). Low wind regimes include wind speeds between 0.0 and 2.0 m s^{-1}, moderate wind regimes include speeds between 2.0 and 5.0 m s^{-1}, and high wind regimes include speeds between 5.0 and 10 m s^{-1}. All results were reported as average ± standard deviation or as indicated.

3. Results

3.1 FDOM concentration and enrichment in the SML

Results regarding the FDOM concentrations in both the SML and bulk water, as well as other physical parameters such as temperature, salinity, and wind speed, are provided for all four stations in **Table 1**. Mean station HPT at a depth of <2 cm ranged between 12.222°C at UP3 and 19.720°C at TF0271 (**Table 1**). The difference of 7.498°C indicates intense upwelling of cold water off the coastline. Mean FDOM concentration in the bulk water did not correlate with bulk salinity (p = 0.7500, r = 0.4000, n = 4; Figure S1a) recorded by the ship's salinometer, but the number of stations was low and the sampled water masses had similar salinities (mean for all four stations of 6.892 ± 0.065, n = 3348). Terrestrial inputs of FDOM in the Baltic Sea typically occur at salinities below 6 (see

Table 1: Biogeochemical and meteorological data[a] for stations UP3 (upwelling), UP2 and UP4 (upwelling influenced) and TF0271 (non-upwelling). DOI: https://doi.org/10.1525/elementa.242.t1

Parameter	Stations			
	UP3[b]	UP2[b]	UP4	TF0271
Date	08.02.2015	08.03.2015	08.04.2015	08.12.2015
Latitude (°E)	16.65225	16.71038	16.88538	20.03563
Longitude (°N)	56.28476	56.28399	56.29571	57.31229
FDOM (μg L^{-1}), SML	24.7 ± 0.3 (*n* = 712)	22.8 ± 0.7 (*n* = 909)	22.5 ± 1.0 (*n* = 804)	13.9 ± 1.3 (*n* = 923)
FDOM (μg L^{-1}), bulk water	16.5 ± 0.7 (*n* = 712)	16.1 ± 1.2 (*n* = 909)	16.3 ± 0.6 (*n* = 804)	13.1 ± 0.7 (*n* = 923)
FDOM, EF	1.5 ± 0.1 (*n* = 712)	1.4 ± 0.1 (*n* = 909)	1.4 ± 0.1 (*n* = 804)	1.1 ± 0.1 (*n* = 923)
HPT (°C), 2-cm depth	12.222 ± 0.211 (*n* = 712)	14.650 ± 1.522 (*n* = 909)	15.893 ± 0.061 (*n* = 804)	19.720 ± 0.092 (*n* = 923)
HPT (°C), 15-cm depth	12.005 ± 0.133 (*n* = 712)	14.552 ± 1.618 (*n* = 909)	15.863 ± 0.059 (*n* = 804)	19.783 ± 0.092 (*n* = 923)
Salinity, SML	7.13 ± 0.30 (*n* = 712)	NA	NA	7.23 ± 0.12 (*n* = 923)
Salinity, bulk water	NA	NA	NA	7.21 ± 0.18 (*n* = 923)
Photosynthetic yield (F_v/F_m)	0.4 ± 0.1 (*n* = 712)	0.3 ± 0.1 (*n* = 909)	0.3 ± 0.1 (*n* = 804)	0.4 ± 0.1 (*n* = 923)
Wind speed (m s^{-1})	2.4 ± 0.7 (*n* = 120)	3.0 ± 0.7 (*n* = 150)	5.6 ± 0.6 (*n* = 180)	4.6 ± 0.9 (*n* = 29)
Solar radiation (W m^{-2})	465 ± 71 (*n* = 120)	617 ± 210 (*n* = 150)	573 ± 209 (*n* = 180)	114 ± 73 (*n* = 29)
UV index	3.3 ± 0.4 (*n* = 120)	5.0 ± 1.0 (*n* = 150)	3.9 ± 0.9 (*n* = 180)	1.1 ± 0.7 (*n* = 29)
Chl *a* (μg L^{-1}), bulk water	6.1 ± 0.1 (*n* = 4)	8.4 ± 2.5 (*n* = 4)	NA	0.9 ± 0.8 (*n* = 4)
Surfactants (μg Teq L^{-1}), SML	341 ± 22 (*n* = 9)	357 ± 16 (*n* = 10)	NA	455 ± 19 (*n* = 7)
Surfactants (μg Teq L^{-1}), bulk water	337 ± 16 (*n* = 9)	346 ± 18 (*n* = 10)	NA	458 ± 35 (*n* = 7)

[a] Reported as average ± standard deviation (with n value).
[b] From Ribas-Ribas et al. (2017).
NA = Not Available.

Figure 5 in Drozdowska et al., 2015), but no river outflows were proximate to our sampling stations. Therefore, we concluded that terrestrial influences were negligible in our study.

The results presented in **Table 1** indicate that the upwelling region we sampled had higher concentrations of FDOM in the SML (23.2 ± 1.1 μg L^{-1}, n = 2425, for stations UP2, UP3 and UP4 combined) than the non-upwelling region (13.9 ± 0.7 μg L^{-1} for TF0271; **Table 1**). The FDOM concentration in bulk water decreased by approximately 20% from station UP3 to station TF0271, a difference that was statistically significant (Mann-Whitney test, $p < 0.0001$). The FDOM concentration in the SML, however, decreased more strongly over this distance, by approximately 50%. This stronger decrease indicates that EFs at the upwelling stations were higher due to the FDOM concentration in the SML rather than differences in the bulk water concentration. An increasing trend between FDOM enrichment and UV index was also observed (Figure S1c), but the correlation was not significant.

FDOM enrichment in the SML at all stations ranged between 0.8 and 2.2 (n = 3348). A histogram of enrichment factors (**Figure 2**) clearly shows that FDOM was always enriched (EF > 1.0) at the upwelling station, UP3 (median = 1.5), and the upwelling-influenced stations, UP2 (median = 1.5) and UP4 (median = 1.4). Depletion was not observed in the upwelling region at any of the 2425 data points from these three stations.

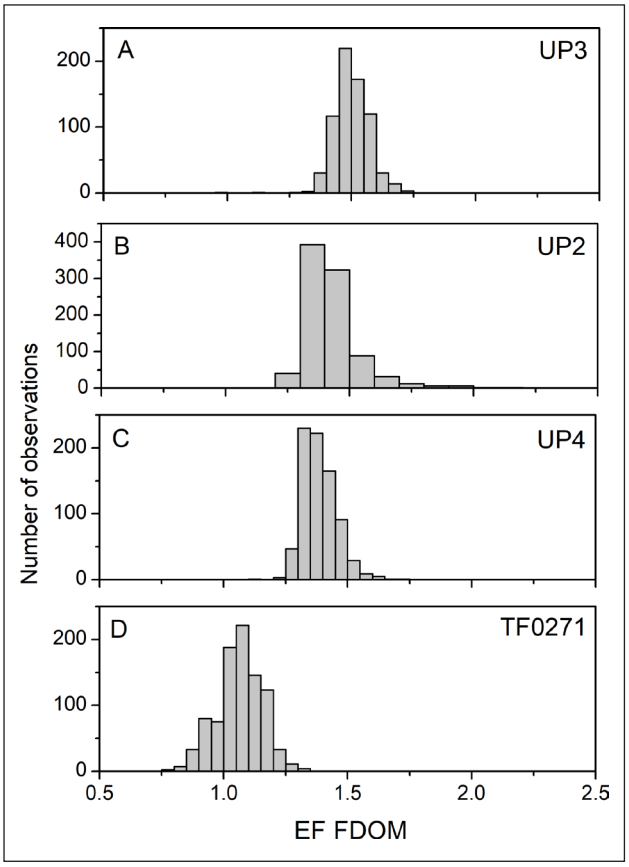

Figure 2: Histogram of FDOM enrichment (EF) in the SML at each station. DOI: https://doi.org/10.1525/elementa.242.f2

The EF of FDOM at the TF0271 station, however, was significantly lower (median = 1.1) compared to the stations in the upwelling region (pooled median = 1.4; Mann-Whitney test, $p < 0.0001$). Of 923 data points from the TF0271 station, 13% indicated that depletion (EF < 1.0) had occurred.

3.2 Biogeochemical and meteorological parameters

The physiological status of photoautotrophic organisms at the UP3 station, represented by photosynthetic yield, was reported by Ribas-Ribas et al. (2017), where the average yield was 0.4 ± 0.1. The UP2 and UP4 stations of this study were similarly characterized with average photosynthetic yields of 0.3 ± 0.1 (**Table 1**). Interestingly, the yield at the TF0271 station (0.4 ± 0.1) was equivalent to that at the upwelling station closest to the shoreline (UP3). However, the Chl *a* concentration, a proxy for biomass, was lower at the TF0271 station (0.9 ± 0.8 μg L^{-1}) than at the UP3 station (6.1 ± 0.1 μg L^{-1}). The concentration of surfactants in the SML, a proxy for the presence of slicks (Wurl et al., 2011b), was significantly higher (Kruskal-Wallis, $p = 0.0045$) at the TF0271 station compared to the UP2 and UP3 stations (**Table 1**). However, in all cases, the concentration was below the 800 μg Teq L^{-1} threshold typically observed for slicks (Wurl et al., 2009). The average wind speed within the upwelling regions increased from UP3 (2.4 ± 0.7 m s^{-1}) to UP4 (5.6 ± 0.6 m s^{-1}). The average wind speed at the TF0271 station was 4.6 ± 0.9 m s^{-1}. Observations in the upwelling region were recorded on a clear day with average solar radiation of 556 ± 201 W m^{-2} (n = 450). Observations at the TF0271 station were recorded on an overcast day with average solar radiation of 114 ± 73 W m^{-2}. During the time on stations in the upwelling region, the average UV index, an indicator of UV radiation (World Health Organization); (WHO, 2002), was 4.1 ± 0.9 (n = 450) compared to 1.1 ± 0.9 (**Table 1**) at the non-upwelling station.

3.3 Variability of FDOM enrichment in the SML

The time series of EFs for stations in the upwelling region are shown in **Figure 3** as one-minute averaged values. In the upwelling region, FDOM was consistently enriched in the SML without a single depletion (EF < 1.0) within a sampling period of 130 minutes. For example, at the UP3 station, we observed 6% variability in FDOM enrichment characterized by the appearance of multiple peaks even as the EF generally decreased over the same period (**Figure 3a**). These peaks appear regularly at intervals of approximately ten minutes. The photosynthetic yield at the UP3 station had similar peaks (e.g., at 09:10 UTC, highlighted as a green line in **Figure 3d**), but at slightly longer intervals; the EF of FDOM showed weak but significant correlation with the yield value ($p = 0.0008$, r = 0.2980). At the UP2 station (**Figure 3b**), the EF of FDOM decreased by 26% during the first 30 minutes of sampling but later showed consistent enrichment over the sampling period. Ribas-Ribas et al. (2017) showed that different water masses, indicated by the presence of a front, led to an increase in FDOM concentration in the underlying bulk water

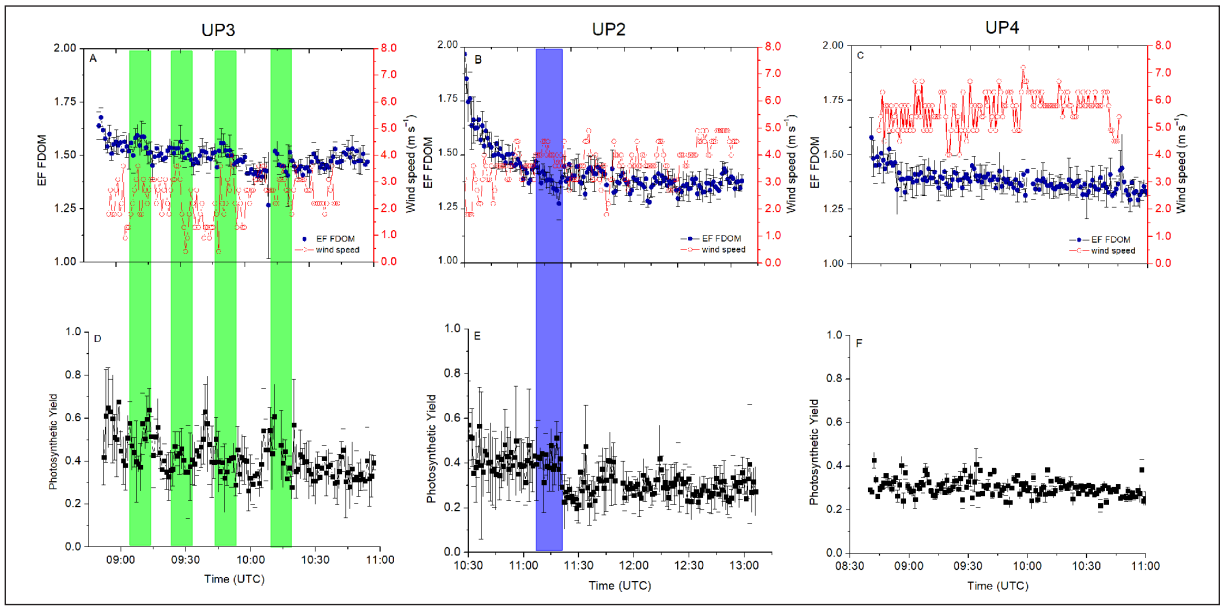

Figure 3: Measurements taken in the upwelling region. Panels **A**, **B** and **C** show EF of FDOM in the SML and wind speed (m s^{-1}) measured at the UP3, UP2, and UP4 stations, respectively. Panels **D**, **E** and **F** show photosynthetic yield (F_v/F_m) at the UP3, UP2, and UP4 stations, respectively. Symbols represent one-minute averages; error bars indicate ± standard deviation (n = 2425). Green shaded bars highlight the enrichment peaks at UP3; the blue shaded bar represents the front area at UP2. DOI: https://doi.org/10.1525/elementa.242.f3

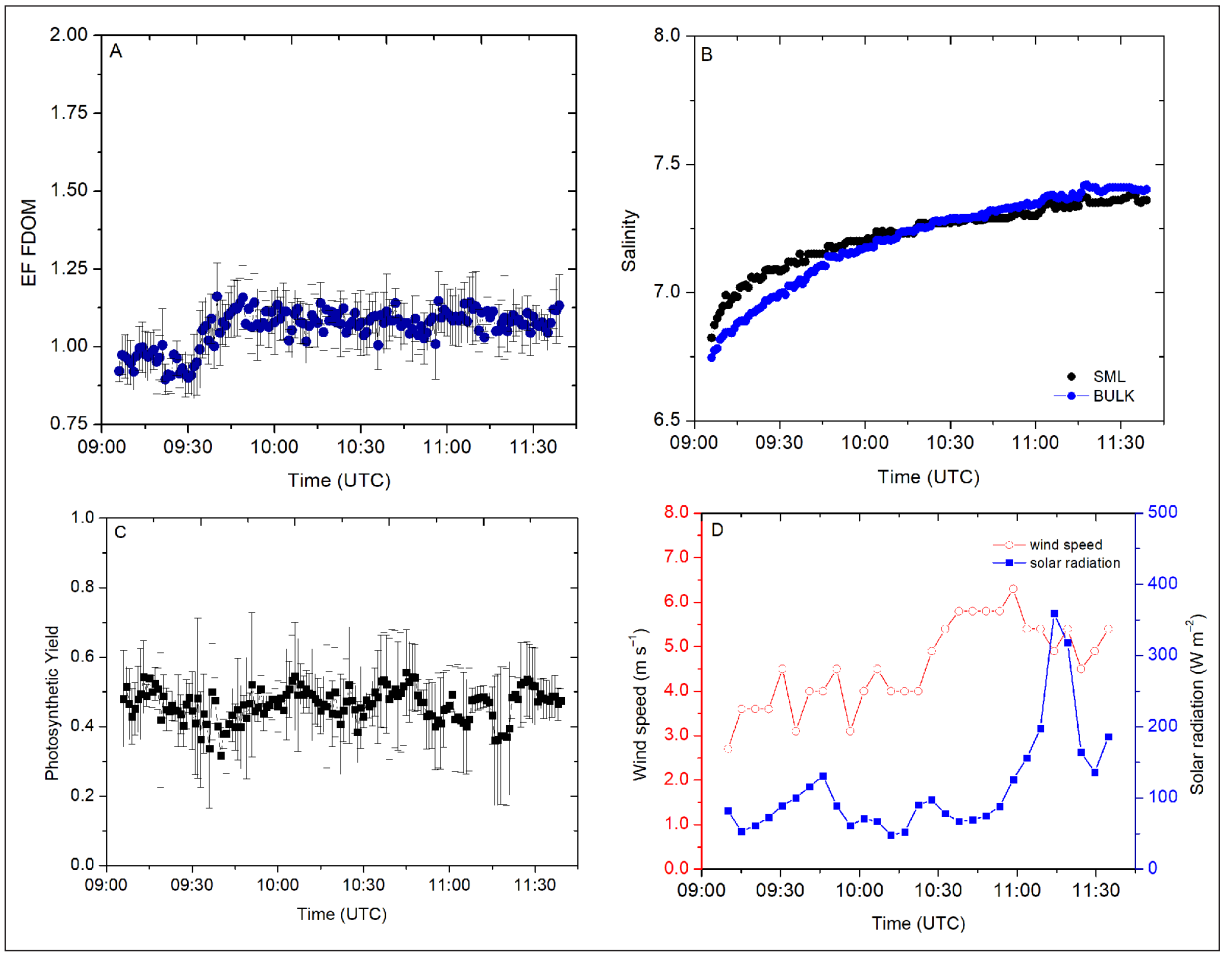

Figure 4: Measurements taken at the TF0271 station. Panels **A**, **B** and **C** show EF of FDOM in the SML, salinity (in both the SML and bulk water) and photosynthetic yield (F_v/F_m), respectively. Symbols represent one-minute averages; error bars indicate ± standard deviation (n = 923). Panel **D** shows wind speed and solar radiation measured in five-minute intervals. DOI: https://doi.org/10.1525/elementa.242.f4

after 11:00 UTC, which in turn led to a decrease in EFs. The UP4 station (**Figure 3c**), which is located 14.1 nautical miles east of the UP3 station, showed a trend of slight decrease in EF over the sampling period of a few hours. At the TF0271 station (**Figure 4**), FDOM was characterized by consistent depletion (EF < 1.0) for the first 30 minutes of sampling (**Figure 4a**). FDOM enrichment then occurred rapidly from 09:30 UTC to 09:45 UTC and continued through the sampling period, though with lower EFs than the other stations, ranging between 1.0 and 1.2. Overall, these observations revealed clear spatiotemporal variability in the EFs of FDOM with distinct patterns, including frequent and regular peaks of enrichment over time at the upwelling station (UP3; **Figure 3a**), a trend of temporally decreasing values at the stations still influenced by but more removed from the upwelling (UP2 and UP4; **Figure 3b** and **3c**), and a rapid increase from depletion to modest enrichment in the absence of upwelling (TF0271, **Figure 4a**).

Presentation of the standard deviations of the one-minute averaged EFs for UP3 (**Figure 5**) and TF0271 (**Figure 6**) as colored points on a plot show the patchiness of FDOM enrichment. The observed standard deviations ranged between ±0.01 μg L^{-1} and ±0.14 μg L^{-1} (median = ±0.04 μg L^{-1}). Low standard deviations (indicated by blue in **Figures 5** and **6**) imply that the EF of FDOM is constant over one minute, whereas high standard deviations (indicated by red in **Figures 5** and **6**) indicate higher fluctuations within one minute corresponding to a few meters on a spatial scale. In comparison, measurements of well-mixed bulk water (contained in a 20-L canister and pumped through the FDOM sensor) revealed a typical standard deviation of ±0.01 μg L^{-1}. We selected two transect areas for both the UP3 and TF0271 stations to assess the short spatiotemporal variability of the EF of FDOM in the SML. At the UP3 station, EFs varied by up to 70% within 50 meters of the transect (**Figure 5b**). Patches of high variability (red color; standard deviation >±0.13 μg L^{-1}) were observed in **Figure 5b**, suggesting that high variability of FDOM can occur within less than five minutes or a few meters. Similar patterns were found in other areas of this transect (**Figure 5c**). Overall, the EF of FDOM observed at the UP3 station showed frequent patchiness in this region with upwelled water. Frequent patchiness was also observed at the UP2 and UP4 stations influenced by upwelling (see Figures S2 and S3), but the absolute changes were not frequent compared to UP3. In contrast, patchiness without upwelled water masses (at TF0271; **Figure 6**) was separated by a larger spatial scale of at least 100 meters. For example, the variability in FDOM enrichment was limited over some 200-meter segments of the transect (**Figure 6b**). In other segments of similar distance (**Figure 6c**), high variability was observed, as indicated by large standard deviations. Although FDOM enrichment at the TF0271 station showed high variability, patchiness occurred less frequently than at the upwelling stations.

3.4 EF of FDOM during different wind regimes

Overall, the range of wind speeds during our observations was 0.5–7.4 m s^{-1}. We examined the frequency of FDOM enrichment during three different wind regimes: low (0.0–2.0 m s^{-1}), moderate (2.0–5.0 m s^{-1}), and high (5.0–10 m s^{-1}), as determined by histograms (**Figure 7**). During the low wind regime, FDOM was consistently enriched (EF ranged from 1.1 to 1.7, with a median value of 1.5). The

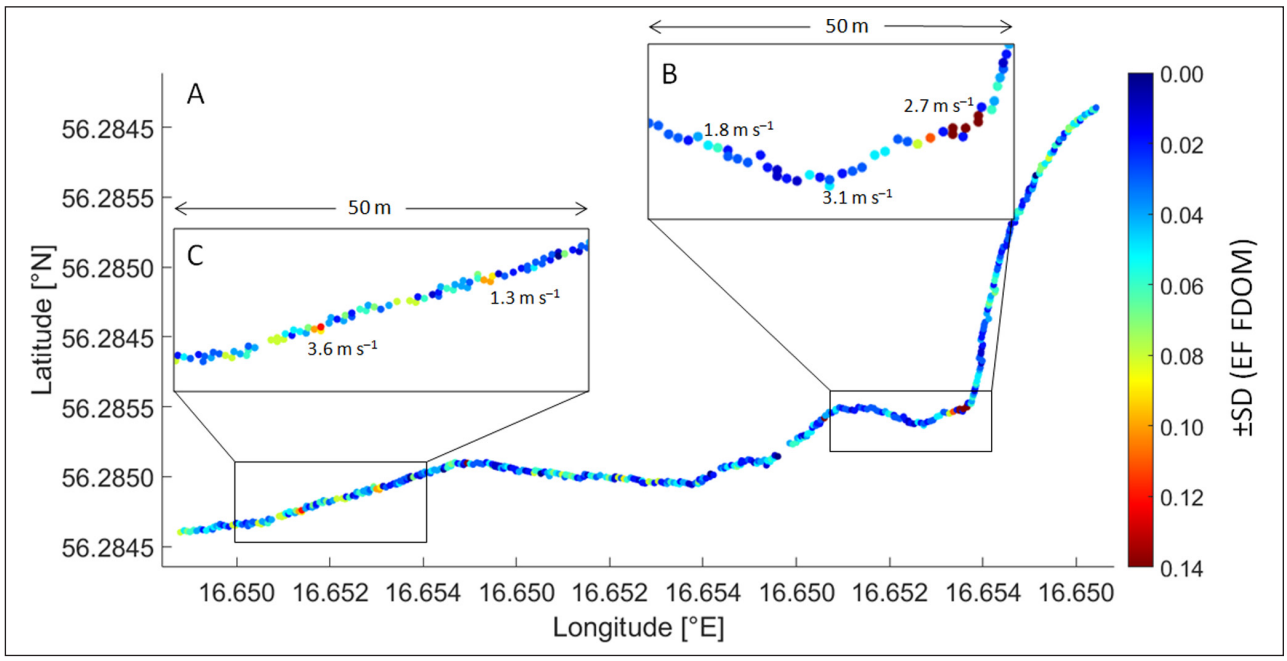

Figure 5: Standard deviation of one-minute average EF at the UP3 station. The distribution of the colored points on the plot **(A)** shows the patchiness of FDOM enrichment. Wind speed (m s^{-1}) is shown on the enlarged insets (**B** and **C**). DOI: https://doi.org/10.1525/elementa.242.f5

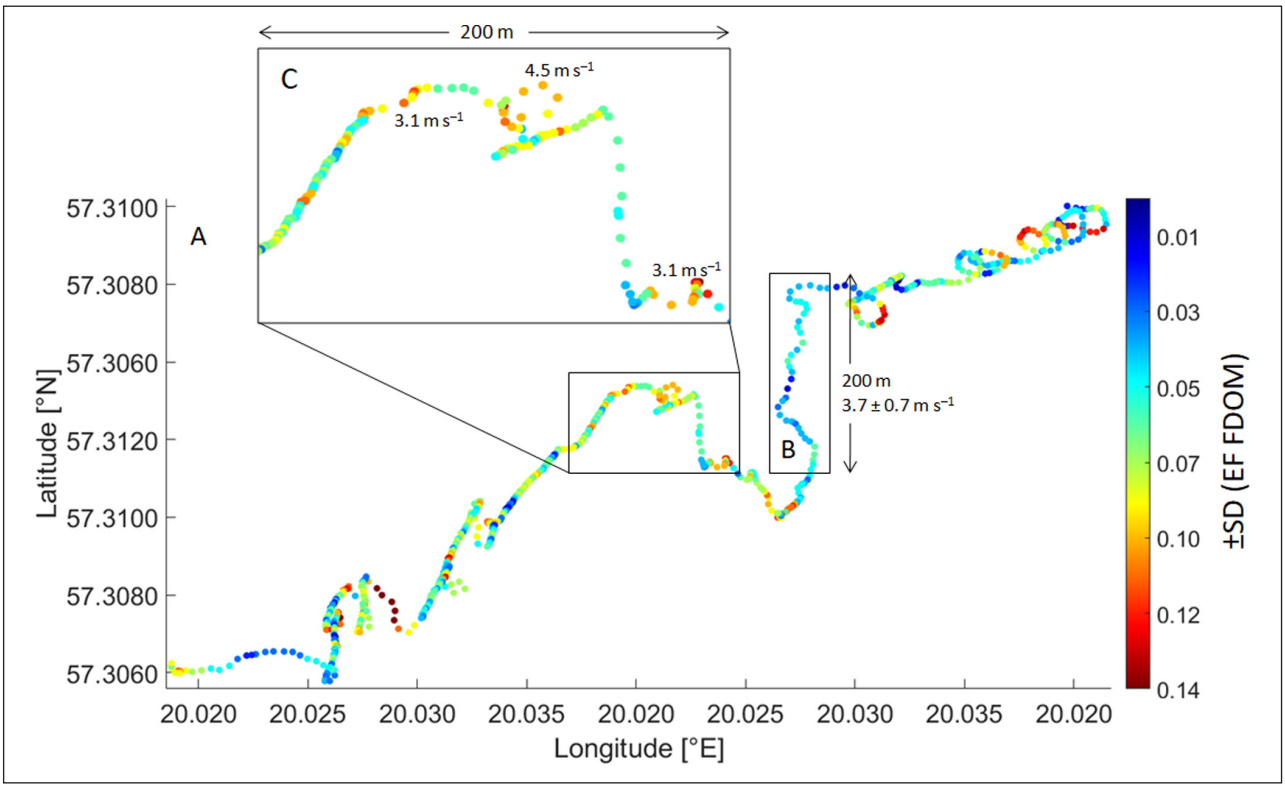

Figure 6: Standard deviation of one-minute average EF at the TF0271 station. The distribution of the colored points on the plot **(A)** show the patchiness of FDOM enrichment. Wind speed (m s^{-1}) is shown for the boxed area of relatively stable EF **(B)** and on the enlarged inset with more dynamic EF **(C)**. DOI: https://doi.org/10.1525/elementa.242.f6

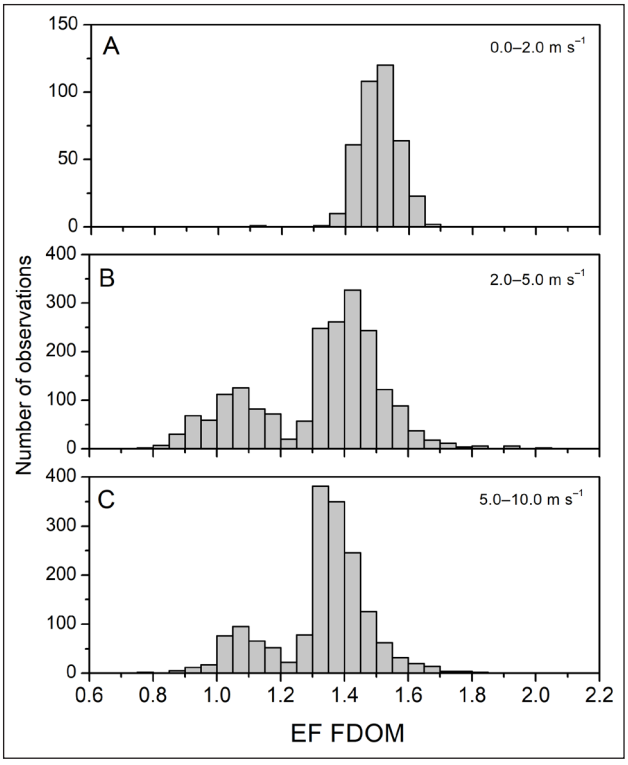

Figure 7: Histrogram of FDOM enrichment (EF) for low, moderate and high wind regimes. (A) Low wind regime was defined as 0.0–2.0 m s^{-1}; **(B)** moderate, as 2.0–5.0 m s^{-1}; and **(C)** high, as 5.0–10 m s^{-1}. DOI: https://doi.org/10.1525/elementa.242.f7

EF had broader distribution during moderate (EF ranged from 0.8 to 2.2) and high wind regimes (EF ranged from 0.6 to 1.8). Depletion occurred at frequencies of 1% and 5% during moderate and high wind regimes, respectively. One-way ANOVA (Kruskal-Wallis test) showed that FDOM enrichment significantly differed during the different wind regimes ($p > 0.001$).

4. Discussion

The results of our study show that (a) the average FDOM concentration in the SML was approximately 50% higher within an upwelling region than in a non-upwelling region, (b) EFs changed in distinct patterns (regular peaks, slow decreasing trends, rapid changes) and (c) patchiness of enrichment on small spatiotemporal scales (<ten meters and <five minutes) is a common feature of the SML. Within the upwelling region we examined, the EFs of FDOM were always enriched (EF: 1.1–2.2, $n = 2425$) in the SML, but in the absence of upwelling (station TF0217) 13% of our data indicated that FDOM was depleted in the SML (EF: 0.8–1.2, $n = 923$). Our results are consistent with Drozdowska et al. (2015) reporting 20% increase in the DOM fluorescence in the SML compared to bulk water. Higher concentrations of amino-acid-like FDOM (excitation range: 250–290 nm, emission range: 320–350 nm) and degree of enrichment (EF: 0.5–3.3, $n = 38$) were reported during an upwelling event off the Peruvian Coast (Galgani and Engel, 2016). Similarly, Frew et al. (2002) reported that the EFs of FDOM (excitation:

355 nm, emission: 450 nm) ranged between 1.0 and 1.7 for non-upwelling region in western North Atlantic, and Wurl et al. (2009) observed EFs between 1.2 and 1.6 (light absorption at 350 nm) in the Pacific. Overall, the range of EF observed in this study for non-upwelled water is similar to these other reports, but a limited number of data points (Galgani and Engel, 2016; $n = 38$) or alternating *in situ* measurements of FDOM in the SML and bulk water (Frew et al., 2002) may have masked some depletion in the previous studies.

The enrichment of organic matter in the SML is generally related to biological processes in the euphotic zone (Hardy, 1982). Organic materials are transported upward from bulk water to the SML through diffusion, positively buoyant particles (Azetsu-Scott and Passow, 2004), and rising air bubbles (Gershey, 1983). In addition to the direct net production of organic matter within the SML (Wurl et al., 2016), upward transport of organic matter from bulk water explains the typical enrichment of organic matter in the SML (Obernosterer et al., 2008). Our observations of elevated EFs during upwelling indicate the ability of upwelled water masses to capture by-products of biological processes from the euphotic zone of the water column. Kitidis et al. (2006) reported a significant correlation between CDOM and Chl *a* in water masses near the sea surface and suggested photoautotrophs as autochthonous sources of CDOM in the open ocean. Nelson et al. (1998) reported that microbial degradation of organic matter also leads to the production of autochthonous CDOM.

Galgani and Engel (2016) suggested that the EF of CDOM in the SML is controlled by microbial release of DOM, including FDOM, which serves as a photo-protective matrix, as described earlier by Tilstone et al. (2010) and Wurl et al. (2011a). The EF of FDOM measured in the upwelling region during our study always showed enrichment, although the average solar radiation (556 ± 201 W m^{-2}) and UV index (4.1 ± 0.9) were relatively high compared to the non-upwelling station (average solar radiation: 114 ± 73 W m^{-2}, UV index: 1.1 ± 0.7). Chen and Bada (1992) reported that surface photo-bleaching of FDOM, which would lead to FDOM depletion in the SML, occurs on timescales of hours during laboratory-based experiments. However, our study and Drozdowska et al. (2015) reported frequent enrichment of FDOM in the SML. Indeed, Tilstone et al. (2010) suggested that microbial production of CDOM, including FDOM, occurs within a well-defined SML, and that CDOM may act as UV-protection for phytoplankton within the SML. Similarly, Obernosterer et al. (2008), who performed their study in a non-upwelling region, reported constant CDOM enrichment in the SML at six stations in the tropical Pacific, providing additional evidence that continuous supply of CDOM to the SML, either from the bulk water or through microbial production in the SML, balances out losses due to photobleaching at extremely high solar and UV irradiance.

Previous studies of CDOM enrichment in the SML focused on the general processes and mechanisms of enrichment (Galgani and Engel, 2016), rather than spatial and temporal variations. Although such processes are highly dynamic at the SML, the short time-scale variability of enrichment in the SML is not well understood (Carlson, 1983). In our study, the EF of FDOM ranged from 1.2 to 1.7 (UP3 station; **Figure 3a**), thus varying by 50% over an observational period of about three hours. This degree of temporal variability indicates that a single observation on EF for a specific study region would be insufficient to understand enrichment processes at the SML. Variability can even occur on a scale of minutes. For example, at the UP3 station, peaks appeared approximately every ten minutes, resulting in 6% variability in the enrichment of FDOM. Although seemingly small, this variability nevertheless indicates that surface renewal, potentially enhanced by advection in upwelling regions (Kermani and Shen, 2009; Thomas et al., 2013), occurs within very short time intervals. At the UP2 station (**Figure 3b**), the temporal decrease in FDOM enrichment was caused by increasing FDOM concentrations in bulk water as the catamaran approached the front (Ribas-Ribas et al., 2017). We attribute the rapid increase in EF from depletion to modest enrichment, observed at the TF0271 station over a 15-minute period (**Figure 4a**), to bulk water mixing with the SML in the same time frame, as indicated by the time series of salinity data (**Figure 4b**) for the SML and bulk water (and by the HPT measurements between depths of 2 and 15 cm; **Table 1**). This conclusion is also supported by significant correlations between the EF of FDOM and salinity in both SML ($p < 0.0001$, $r = 0.3423$) and bulk water ($p < 0.0001$, $r = 0.3417$), despite lack of correlation between concentration of FDOM and salinity in either SML or bulk water. As different water masses contain surface-active materials from various sources (e.g., terrestrial, considered negligible for this study, and autochthonous sources), potentially highly surface-active FDOM material from bulk water may have been brought to the SML at the TF0271 station via mixing.

In addition to temporal variations, high-resolution measurements of FDOM enrichment provide insights into the spatial patchiness of SML characteristics. For example, Frew et al. (2004) suggested that different water masses contribute to changes in the EF of FDOM (calculated from **Table 1** in Frew et al., 2004; EF: 1.0 to 1.8, except at Station 5, where EF = 4.8) between the SML and bulk water at spatial scales of 50 to 200 km (estimated from **Figure 1** in Frew et al., 2004). We showed that EFs changed from 0.8 to 1.1 (**Figure 4a**) on the much smaller spatial scale of < 200 meters due to the mixing of water masses. Our study took place on a spatial scale similar to that of Frew et al. (2002), who reported a complex pattern of EF fluctuations on spatial scales of 10 to 1000 meters. This pattern was attributed to banded slicks frequently crossed by the deployed catamaran at low to moderate wind speeds (0.5–4.5 m s^{-1}). At UP3, we observed several patches of highly variable enrichment of FDOM (**Figure 5b** and **c**) within a few meters (and <two minutes). However, the concentration of surfactants in the SML was too low (between 341 ± 22 and 455 ± 19 μg Teq L^{-1}; **Table 1**) to indicate the presence of slicks. For example, Wurl et al. (2009) reported surfactant concentrations in slick samples ranging between 784 and 1962 μg Teq L^{-1}. The high variability of EF in FDOM, shown as red patches in **Figures 5** and **6**, may correspond to patches of floating particulate material

trapped by surface tension within the SML (Hunter, 1980). The average wind speed (2.4 ± 0.7 m s^{-1}, **Table 1)** observed at the UP3 station was within the low wind regime, which would allow for floatation of particles at the sea surface. High variability of FDOM enrichment, indicated by high standard deviations, was also observed at TF0271 (non-upwelling station; **Figure 6a**). Patchiness in non-upwelling regions occurred at larger spatial scales (approximately 200 meters) with both low (**Figure 6b**) and high variability (**Figure 6c**) compared to upwelling regions (**Figure 5b** and **c**). Mahadevan and Campbell (2002) showed that the small-scale variability in the surface concentration of Chl *a* within an upwelling region occurred at a smaller scale than that associated with horizontal advection. Our observation that FDOM enrichment was more variable at smaller scales during upwelling is consistent with their work. Frew et al. (2004) pointed out that the patchiness of SML distribution was associated with the frequency of surface renewal due to localized forcing and upwelling, a conclusion also supported by our observations.

One of the apparent localized forces is wind speed, which has a dynamic force on the sea surface. Even though no clear relationship between EF of surface-active DOM and wind speed was detected by Wurl et al. (2011b), they found distinct ranges in the EF of surface-active DOM in the same wind regimes reported in our study. Based on the histogram shown in **Figure 7**, we found that FDOM was enriched in the SML without depletion during a low wind regime, probably due to the stability of the surface film which would have allowed organic matter, including FDOM, to accumulate at the SML. During moderate to high wind regimes, Frew et al. (2004) found that breaking waves disrupted the surface and physically drove organic matter back to the bulk water, resulting in lower EFs. Our results showed that FDOM remained enriched even in a higher wind regime (5.0–10 m s^{-1}), consistent with the findings of Wurl et al. (2011b). At the UP2 station (**Figure 3b**), decreases in the EF of FDOM were observed with increasing wind speeds for the first 30 minutes. However, the presence of a front (Ribas-Ribas et al., 2017) indicates that both different water masses and increasing wind influenced the decreasing EFs at this station. Increasing wind speeds (from 4.9 to 7.2 m s^{-1}) were observed with a slightly decreasing trend of FDOM enrichment at the UP4 station (**Figure 3c**). Although Frew et al. (2002) associated the small-scale variability of FDOM enrichment with wind speed and wave slope, we observed that low variability of FDOM enrichment was not always associated with low wind speeds. In our study, wind speeds were above the threshold for micro-breaking of waves (2.5 m s^{-1}); (Hwang and Sletten, 2008), but the variability of enrichment was very low (± 0.02 μg L^{-1}; **Figure 5b**). Similarly, low variability at the TF0271 station occurred with an average wind speed of 3.7 ± 0.7 m s^{-1} (**Figure 6b**). High variability occurred not only when wind speeds were above 2.5 m s^{-1} but also during low wind speeds (1.3 m s^{-1}), as shown in **Figure 5c**. Overall, we recognize that wind speed may play a role in controlling the enrichment of FDOM in the SML, but expecting to obtain a simple (one-factor) understanding of enrichment may not be reasonable given the multiple complex processes involved, including photochemical processes driven by solar and UV radiation, mixing, upwelling of water masses, and biological processes as a source of FDOM.

5. Conclusions

The results of our high-resolution investigation of FDOM enrichment in the SML and its spatiotemporal variability in upwelling and non-upwelling regions of the Baltic Sea lead to several conclusions. In upwelling water masses, FDOM was consistently enriched in the SML despite highest radiation levels observed, from which we conclude that upwelling continuously supplies and sustains the concentration of FDOM to the SML. The EF of FDOM in the SML demonstrated 6% variability within intervals of less than ten minutes. We conclude that the enrichment of FDOM in the SML is patchy and, further, that the pattern of patchiness varies in the presence of upwelling due to enhanced surface renewal rates. We also found that wind speed skewed the distribution of EF and that mixing processes caused rapid changes in EF. We conclude that multiple environmental parameters affect the complex processes involved in enrichment. Overall, our high-resolution measurements of FDOM in the SML show how such information can be used to gain a better mechanistic understanding of enrichment processes at this critical interface between the ocean and atmosphere.

Data Accessibility Statement

Data in this study has been submitted to PANGAEA DOI: https://doi.org/110.1594/PANGAEA.868976.

Supplemental Files

The supplemental files for this article can be found as follows:

- **Figure S1.** Correlations between salinity and FDOM (bulk and EF) and between UV index and EF FDOM. DOI: https://doi.org/10.1525/elementa.242.s1
- **Figure S2.** Standard deviation of one-minute average EF at the UP2 station. DOI: https://doi.org/10.1525/elementa.242.s2
- **Figure S3.** Standard deviation of one-minute average EF at the UP4 station. DOI: https://doi.org/10.1525/elementa.242.s3

Acknowledgements

We would like to thank the Crew of the *R/V Meteor* for assistance during the M117 cruise. We appreciate the help from J. Rahlff, M. Laderhoff, and M. van Pinxteren, during sampling.

Funding information

This research was funded by European Research Council (ERC; contract GA336408).

Competing interests

The authors have no competing interests to declare.

Author contributions

- Contributed to conception and design: OW
- Contributed to acquisition of data: NIHM, MRR, OW

- Contributed to analysis and interpretation of data: NIHM, MRR
- Drafted and/or revised the article: NIHM, OW
- Approved the submitted version for publication: OW, MRR, NIHM

References

Azetsu-Scott, K and **Passow, U** 2004 Ascending marine particles: Significance of transparent exopolymer particles (TEP) in the upper ocean. *Limnol Oceanogr* **49**(3): 741–748. DOI: https://doi.org/10.4319/lo.2004.49.3.0741

Blough, N 2005 Photochemistry in the sea-surface microlayer. In: Liss, PS and Duce, RA (eds.), *The Sea-Surface and Global Change*, 383–424. Cambridge University Press.

Carlson, DJ 1983 Dissolved organic materials in surface microlayers: Temporal and spatial variability and relation to sea state. *Limnol Oceanogr* **28**(3): 415–431. DOI: https://doi.org/10.4319/lo.1983.28.3.0415

Carlson, DJ 1993 The early diagenesis of organic matter: Reaction at the air-sea interface. In: Engel, MH and Macko, SA (eds.), *Organic Geochemistry: Principles and Applications,* 255–268. Boston, MA: Springer US. DOI: https://doi.org/10.1007/978-1-4615-2890-6_12

Chen, RF and **Bada, JL** 1992 The fluorescence of dissolved organic matter in seawater. *Mar Chem* **37**(3): 191–221. DOI: https://doi.org/10.1016/0304-4203(92)90078-O

Clemente-Colon, P and **Xiao-Hai, Y** 1999 Observations of East Coast upwelling conditions in synthetic aperture radar imagery. *IEEE T Geosci Remote* **37**(5): 2239–2248. DOI: https://doi.org/10.1109/36.789620

Coble, PG 2007 Marine optical biogeochemistry: The chemistry of ocean color. *Chem Rev* **107**(2): 402–418. DOI: https://doi.org/10.1021/cr050350

Ćosović, B and **Vojvodić, V** 1998 Voltammetric analysis of surface active substances in natural seawater. *Electroanalysis* **10**(6): 429–434. DOI: https://doi.org/10.1002/(SICI)1521-4109(199805)10:6<429::AID-ELAN429>3.0.CO;2-7

Cunliffe, M, Engel, A, Frka, S, Gašparović, B, Guitart, C, et al. 2013 Sea surface microlayers: A unified physicochemical and biological perspective of the air–ocean interface. *Prog Oceanogr* **109**: 104–116. DOI: https://doi.org/10.1016/j.pocean.2012.08.004

Cunliffe, M, Whiteley, AS, Newbold, L, Oliver, A, Schäfer, H, et al. 2009 Comparison of bacterioneuston and bacterioplankton dynamics during a phytoplankton bloom in a fjord mesocosm. *Appl Environ Microbiol* **75**(22): 7173–7181. DOI: https://doi.org/10.1128/AEM.01374-09

de Bruyn, WJ, Clark, CD, Pagel, L and **Takehara, C** 2011 Photochemical production of formaldehyde, acetaldehyde and acetone from chromophoric dissolved organic matter in coastal waters. *J Photochem Photobiol A: Chem* **226**(1): 16–22. DOI: https://doi.org/10.1016/j.jphotochem.2011.10.002

Dragcevic, D and **Pravdic, V** 1981 Properties of the seawater-air interface. 2. Rates of surface film formation under steady state conditions1. *Limnol Oceanogr* **26**(3): 492–499. DOI: https://doi.org/10.4319/lo.1981.26.3.0492

Drozdowska, V, Kowalczuk, P and **Jozefowicz, M** 2015 Spectrofluorometric characteristics of fluorescent dissolved organic matter in a surface microlayer in the Southern Baltic coastal waters. *J Eur Opt Soc – Rapid* **10**. DOI: https://doi.org/10.2971/jeos.2015.15050

Frew, NM, Bock, EJ, Schimpf, U, Hara, T, Haußecker, H, et al. 2004 Air-sea gas transfer: Its dependence on wind stress, small-scale roughness, and surface films. *J Geophys Res-Oceans* **109**(C8). DOI: https://doi.org/10.1029/2003JC002131

Frew, NM, Nelson, RK, McGillis, WR, Edson, JB, Bock, EJ, et al. 2002 Spatial variations in surface microlayer surfactants and their role in modulating air-sea exchange. In: Donelan, M, Drennan, W, Saltzman, E and Wanninkhof, R (eds.), *Gas Transfer at Water Surfaces,* 153–159. Washington, D.C.: American Geophysical Union Press. DOI: https://doi.org/10.1029/GM127p0153

Galgani, L and **Engel, A** 2016 Changes in optical characteristics of surface microlayers hint to photochemically and microbially mediated DOM turnover in the upwelling region off the coast of Peru. *Biogeosciences* **13**(8): 2453–2473. DOI: https://doi.org/10.5194/bg-13-2453-2016

Gershey, RM 1983 Characterization of seawater organic matter carried by bubble-generated aerosols. *Limnol Oceanogr* **28**(2): 309–319. DOI: https://doi.org/10.4319/lo.1983.28.2.0309

Hardy, JT 1982 The sea surface microlayer: Biology, chemistry and anthropogenic enrichment. *Prog Oceanogr* **11**(4): 307–328. DOI: https://doi.org/10.1016/0079-6611(82)90001-5

Hunter, K 1980 Processes affecting particulate trace metals in the sea surface microlayer. *Mar Chem* **9**(1): 49–70. DOI: https://doi.org/10.1016/0304-4203(80)90006-7

Hwang, PA and **Sletten, MA** 2008 Energy dissipation of wind-generated waves and whitecap coverage. *J Geophys Res-Oceans* **113**(2). DOI: https://doi.org/10.1029/2007JC004277

Kermani, A and **Shen, L** 2009 Surface age of surface renewal in turbulent interfacial transport. *Geophys Res Lett* **36**(10). DOI: https://doi.org/10.1029/2008GL037050

Kieber, DJ, McDaniel, J and **Mopper, K** 1989 Photochemical source of biological substrates in sea water: implications for carbon cycling. *Nature* **341**(6243): 637–639. DOI: https://doi.org/10.1038/341637a0

Kitidis, V, Stubbins, AP, Uher, G, Upstill Goddard, RC, Law, CS, et al. 2006 Variability of chromophoric organic matter in surface waters of the Atlantic Ocean. *Deep-Sea Res Pt II* **53**(14–16): 1666–1684. DOI: https://doi.org/10.1016/j.dsr2.2006.05.009

Liss, PS and **Duce, RA** 2005 *The sea surface and global change*. Cambridge University Press.

Lorenzen, CJ 1967 Determination of chlorophyll and pheo-pigments: Spectrophotometric equations. *Limnol Oceanogr* **12**(2): 343–346. DOI: https://doi.org/10.4319/lo.1967.12.2.0343

Mahadevan, A and **Campbell, J** 2002 Biogeochemical patchiness at the sea surface. *Geophys Res Lett* **29**(19). DOI: https://doi.org/10.1029/2001GL014116

Nelson, N, Siegel, D and **Michaels, A** 1998 Seasonal dynamics of colored dissolved material in the Sargasso Sea. *Deep-Sea Res Pt I* **45**(6): 931–957. DOI: https://doi.org/10.1016/S0967-0637(97)00106-4

Obernosterer, I, Catala, P, Lami, R, Caparros, J, Ras, J, et al. 2008 Biochemical characteristics and bacterial community structure of the sea surface microlayer in the South Pacific Ocean. *Biogeosciences* **5**(3): 693–705. DOI: https://doi.org/10.5194/bg-5-693-2008

Pierson, WJ and **Moskowitz, L** 1964 A proposed spectral form for fully developed wind seas based on the similarity theory of SA Kitaigorodskii. *J Geophys Res* **69**(24): 5181–5190. DOI: https://doi.org/10.1029/JZ069i024p05181

Ribas-Ribas, M, Mustaffa, NIH, Rahlff, J, Stolle, C and **Wurl, O** 2017 Sea Surface Scanner (S^3): A catamaran for high-resolution measuremnets of biochemical properties of the sea surface microlayer. *J Atmos Oceanic Technol* **34**: 1433–1448. DOI: https://doi.org/10.1175/JTECH-D-17-0017.1

Shinki, M, Wendeberg, M, Vagle, S, Cullen, JT and **Hore, DK** 2012 Characterization of adsorbed microlayer thickness on an oceanic glass plate sampler. *Limnol Oceanogr Methods* **10**: 728–735. DOI: https://doi.org/10.4319/lom.2012.10.728

Stolle, C, Nagel, K, Labrenz, M and **Jürgens, K** 2010 Succession of the sea-surface microlayer in the coastal Baltic Sea under natural and experimentally induced low-wind conditions. *Biogeosciences* **7**(9): 2975. DOI: https://doi.org/10.5194/bg-7-2975-2010

Thomas, LC, Padmakumar, K, Smitha, B, Devi, CA, Nandan, SB, et al. 2013 Spatio-temporal variation of microphytoplankton in the upwelling system of the south-eastern Arabian Sea during the summer monsoon of 2009. *Oceanologia* **55**(1): 185–204. DOI: https://doi.org/10.5697/oc.55-1.185

Tilstone, GH, Vicente, VM, Widdicombe, C and **Llewellyn, C** 2010 High concentrations of mycosporine-like amino acids and colored dissolved organic matter in the sea surface microlayer off the Iberian Peninsula. *Limnol Oceanogr* **55**(5): 1835–1850. DOI: https://doi.org/10.4319/lo.2010.55.5.1835

WHO 2002 *Global Solar UV Index: A Practical Guide*. Geneva: World Health Organisation.

Williams, P, Carlucci, A, Henrichs, S, Van Vleet, E, Horrigan, S, et al. 1986. Chemical and microbiological studies of sea-surface films in the Southern Gulf of California and off the West Coast of Baja California. *Mar Chem* **19**(1): 17–98. DOI: https://doi.org/10.1016/0304-4203(86)90033-2

Wurl, O, Miller, L, Röttgers, R and **Vagle, S** 2009 The distribution and fate of surface-active substances in the sea-surface microlayer and water column. *Mar Chem* **115**(1): 1–9. DOI: https://doi.org/10.1016/j.marchem.2009.04.007

Wurl, O, Miller, L and **Vagle, S** 2011a Production and fate of transparent exopolymer particles in the ocean. *J Geophys Res-Oceans* **116**(C7). DOI: https://doi.org/10.1029/2011JC007342

Wurl, O, Stolle, C, Van Thuoc, C, The Thu, P and **Mari, X** 2016 Biofilm-like properties of the sea surface and predicted effects on air-sea CO_2 exchange. *Prog Oceanogr* **144**: 15–24. DOI: https://doi.org/10.1016/j.pocean.2016.03.002

Wurl, O, Wurl, E, Miller, L, Johnson, K and **Vagle, S** 2011b Formation and global distribution of sea-surface microlayers. *Biogeosciences* **8**(1): 121–135. DOI: https://doi.org/10.5194/bg-8-121-2011

Yamashita, Y and **Tanoue, E** 2009 Basin scale distribution of chromophoric dissolved organic matter in the Pacific Ocean. *Limnol Oceanogr* **54**(2): 598–609. DOI: https://doi.org/10.4319/lo.2009.54.2.0598

Yu, L 2010 On sea surface salinity skin effect induced by evaporation and implications for remote sensing of ocean salinity. *J Phys Oceanogr* **40**(1): 85–102. DOI: https://doi.org/10.1175/2009JPO4168.1

Zhang, J and **Yang, G** 2013 Chemical properties of colored dissolved organic matter in the sea-surface microlayer and subsurface water of Jiaozhou Bay, China in autumn and winter. *Acta Oceanol Sin* **32**(6): 26–39. DOI: https://doi.org/10.1007/s13131-013-0306-4

Zhang, Z, Cai, W, Liu, L, Liu, C and **Chen, F** 2003 Direct determination of thickness of sea surface microlayer using a pH microelectrode at original location. *Science in China Series B: Chemistry* **46**(4): 339–351. DOI: https://doi.org/10.1360/02yb0192

How to cite this article: Mustaffa, NIH, Ribas-Ribas, M and Wurl, O 2017 High-resolution variability of the enrichment of fluorescence dissolved organic matter in the sea surface microlayer of an upwelling region. *Elem Sci Anth,* 5: 52, DOI: https://doi.org/10.1525/elementa.242

Domain Editor-in-Chief: Jody W. Deming, University of Washington, US

Knowledge Domain: Ocean Science

Part of an *Elementa* Special Feature: The sea surface microlayer

Submitted: 28 February 2017 **Accepted:** 03 August 2017 **Published:** 11 September 2017

Copyright: © 2017 The Author(s). This is an open-access article distributed under the terms of the Creative Commons Attribution 4.0 International License (CC-BY 4.0), which permits unrestricted use, distribution, and reproduction in any medium, provided the original author and source are credited. See http://creativecommons.org/licenses/by/4.0/.

ELEMENTA Science of the Anthropocene

Elem Sci Anth is a peer-reviewed open access journal published by University of California Press.

OPEN ACCESS